

# Commissioning of the tuned DC readout at GEO 600

J. Degallaix<sup>1</sup>, H. Grote<sup>1</sup>, M. Prijatelj<sup>1</sup>, M. Hewitson<sup>1</sup>, S. Hild<sup>2,3</sup>, C. Affeldt<sup>1</sup>, A. Freise<sup>2</sup>, J. Leong<sup>1</sup>, H. Lück<sup>1</sup>, K. A. Strain<sup>1,3</sup>, H. Wittel<sup>1</sup>, B. Willke<sup>1</sup> and K. Danzmann<sup>1</sup>

<sup>1</sup> Max-Planck-Institut für Gravitationsphysik (Albert-Einstein-Institut) and Leibniz Universität Hannover, Callinstr. 38, 30167 Hannover, Germany

<sup>2</sup> School of Physics and Astronomy, The University of Birmingham, Edgbaston, Birmingham, B15 2TT, United Kingdom

<sup>3</sup> Institute for Gravitational Research, University of Glasgow, Glasgow, G12 8QQ, United Kingdom, United Kingdom

E-mail: jerome.degallaix@aei.mpg.de

## Abstract.

Recent experimental results from GEO600 operating with a DC readout and a tuned signal recycling cavity are reported. Compared to the S5/Astrowatch setup, two major changes in the configuration have been implemented: the control readout to keep the interferometer on the dark fringe is changed from heterodyne to homodyne readout and the signal recycling cavity is shifted from a 550 Hz detuning to a 0 Hz detuning (also called tuned). As preliminary experiments showed, the tuned DC readout sensitivity is similar to the heterodyne one. To take advantage of the new DC readout detection scheme, an Output Mode Cleaner (OMC) has to be installed. The design, building and testing of the GEO OMC, which consists of a 4 mirrors monolithic ring cavity, will also be presented in this article.

## 1. Introduction

The transition between GEO [1] and GEO-HF [2] will be achieved after the completion of several major upgrades. Among those upgrades, the error signal used to keep the interferometer on the dark fringe will no longer be derived from a heterodyne readout but from a homodyne detection scheme called DC readout. The advantages of DC readout over heterodyne readout are numerous [3] but the full benefits of this technique can only be achieved with the presence of an Output Mode Cleaner (OMC). At the same time as changing the readout technique, the GEO signal recycling cavity resonance will be shifted from 550 Hz (detuned case) to 0 Hz (tuned case). This shift of the signal recycling mirror lowers the contribution of most technical noises to the sensitivity [4] and it allows a frequency independent injection of broadband squeezed light in order to lower the shot noise limited sensitivity [5].

Experimentally, the advantage of DC readout has first been reported by the 40m prototype interferometer at Caltech [6]. Regarding GEO, the motivation and technicality of tuned DC readout have also already been published [3] and will not be reminded here.

This paper is part of a series of articles about the recent development of GEO 600. Additional details regarding the interferometer can be found in the following papers. The meaning of Astrowatch as well as a comparison of the GEO noise budget for heterodyne and homodyne

readout is reported by Grote [7]. The longitudinal control and the autoalignment of the output mode cleaner is described in Prijatelj *et al.* [8]. Finally for the long term vision and to understand the role of tuned DC readout in GEO-HF, the reader can refer to Lück *et al.* [9].

This article, about the preparation of tuned DC readout for GEO-HF, is divided into two parts. In the first part, the experiments and the preliminary sensitivity of GEO in a tuned DC readout configuration are reported. The second part is about the design and the building of the output mode cleaner which has been tested in the Albert Einstein Institute in Hannover before being installed at the GEO site.

## 2. Experimental results of tuned DC readout

### 2.1. Background

From November 2007 to July 2009, GEO participated in Astrowatch while the LIGO (4k) and Virgo interferometers were being upgraded. GEO achieved its Astrowatch mission with a duty cycle of more than 85%. This high duty cycle was possible due to restrictions placed on commissioning. Only reversible and limited hardware changes were permitted and were carried out during the day in such a way as to allow the detector to operate in low noise condition over the nights and weekends. Even with these constraints, we managed to stably lock on tuned DC readout to further investigate this configuration.

Due to Astrowatch, we were not able to test the complete DC readout setup planned for GEO-HF. In particular, we did not have an OMC installed, so the higher order optical modes and the modulation sideband fields were still present at the dark port with large amplitudes (contributing a few tens of milliwatts to the detected power). As a result, for the carrier field from the dark fringe offset to dominate the dark port, two actions had to be taken. First, the modulation index of the Michelson sidebands was reduced, reducing the power of the sidebands by a factor 50. Secondly, a large dark fringe offset of 20 pm was implemented.

### 2.2. Lock acquisition

It would have taken too long to develop a new locking procedure to directly lock to tuned signal recycling and DC readout, so it was naturally decided to first lock the interferometer using detuned heterodyne readout. Thus, the same robust locking script implemented for the previous S5/Astrowatch configuration is also used for DC readout.

After the interferometer is locked with a detuned signal recycling and a low laser input power, the metamorphosis to DC readout can begin. First, control of the interferometer's longitudinal degree of freedom is shifted from low noise photodiodes to photodiodes with large dynamical which are detecting attenuated beams. Second, the signal recycling mirror is (abruptly) shifted from the detuned position to the tuned one [4]. Third, the RF modulation index is reduced and the gains of the different control loops are adjusted to compensate. Fourth, a dark fringe offset is introduced that, together with the reduced RF sideband power, ensures the fundamental mode dominates the dark port power. Fifth, the dark fringe control is shifted from the heterodyne to the DC readout error signal. And, finally, the input laser power is increased to the nominal power."

Presently, during normal weather conditions, the success rate of going from detuned heterodyne to tuned DC readout is around 70%. The most critical steps of the locking procedure are the controlled jump of the signal recycling mirror from detuned to tuned position and the switching on of the DC control with the high power photodiode.

### 2.3. The DC readout sensitivity

The sensitivity achieved for tuned DC readout is presented in figure 1. Compared to the heterodyne sensitivity which has been used since the beginning of GEO and so has been heavily

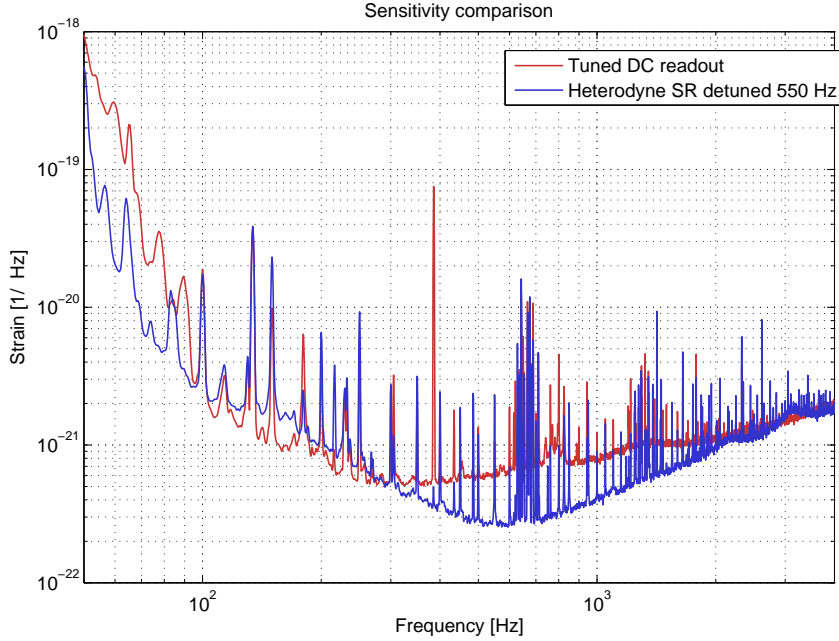


**Figure 1.** Sensitivity comparison between the preliminary tuned DC readout configuration and the heterodyne readout used during S5 and Astrowatch.

optimised and tested, the sensitivity of tuned DC readout is promising. We obtained a better sensitivity in tuned DC readout compared to heterodyne readout in the frequency range from 100 Hz to 300 Hz and similar sensitivity at high frequencies above 2 kHz, where the sensitivity is limited by the shot noise.

For frequencies below 100 Hz, where we are limited by the Michelson autoalignment feedback noise, DC readout yields a slightly worse sensitivity. That is a direct consequence of the reduction of the sideband amplitude since these sidebands are also used to derive the alignment error signal from the differential wavefront sensing scheme. The decrease in the sideband power is compensated by an increase in the autoalignment gain resulting in higher noise at low frequency, due to the amplification of the electronic noise.

In the frequency range between 300 Hz and 2 kHz, the preliminary tuned DC sensitivity is worse compared to the heterodyne readout. That is not fully understood but recently this noise has been greatly decreased (not shown here but present in [7]) with better stabilization of the sidebands and by placing the detection photodiode inside a closed vacuum tank (but still in air).

#### 2.4. Noise budget

The noise budget of tuned DC readout is presented in figure 2. As mentioned earlier, at low frequencies (below 100 Hz) we are limited by the autoalignment feedback noise. In the middle frequency range, the dominant known noise source is the laser amplitude noise. As in the case of heterodyne readout, the noise budget does not explain fully the measured sensitivity since a gap is remaining between the sum of the projected noise and the sensitivity. The large coupling of laser amplitude noise is a direct consequence of the dark fringe offset. And at high frequencies, the sensitivity is shot noise limited.

Compared to detuned heterodyne readout, the tuned DC readout scheme lowers the coupling of several technical noises to the sensitivity as shown in figure 3. The transfer functions presented here can simply simply be understood as the sensitivity curve divided by the noise spectra. The

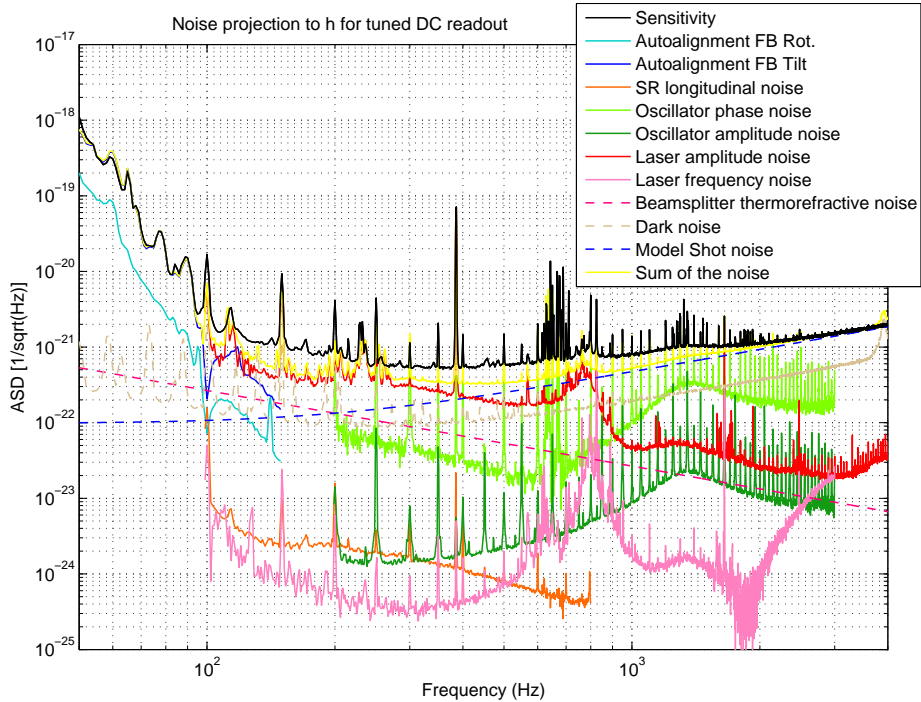


**Figure 2.** Noise budget of the tuned DC readout configuration.

absolute magnitude of the transfer functions is arbitrary since it depends how the noise is detected and then recorded. However the noise detection process is common to heterodyne and DC readout, so a relative comparison of the 2 configurations is still meaningful.

The noise transfer functions of the signal recycling longitudinal actuator, of the laser frequency noise, and of the sidebands oscillator amplitude noise (not shown) are reduced by a factor up to 10. The sidebands oscillator phase noise transfer function has roughly the same level but with different features. Only the coupling of the laser amplitude noise appears higher in the new configuration.

In DC readout, the laser laser amplitude noise couples stronger to the sensitivity than in heterodyne readout. To be explained, it must first be reminded that the calibrated strain sensitivity curve is derived from the error signal used to keep the Michelson interferometer on the dark fringe. For the DC readout configuration, this error signal is simply the power spectra of the light detected at the dark port and so is also a direct measurement of the input laser amplitude [10] (minus the low pass filtering effect of the power recycling cavity). Moreover, the use of a dark fringe offset also reduce the common mode rejection from the Michelson interferometer, increasing slightly the level of the laser amplitude noise at the dark port.

For GEO-HF, we expect an improvement in the sensitivity compared to the one presented here since after the installation of the OMC, a smaller dark fringe offset will be implemented and the sidebands will be restored to their optimal amplitudes while not reaching the detection photodiode.

### 3. The GEO 600 output mode cleaner

During the installation of GEO-HF, the input laser will be upgraded and up to 10 times more light will circulate in the interferometer compared to the present GEO setup. Due to the presence of higher order modes and of the sidebands fields kept for the autoalignment system, more than

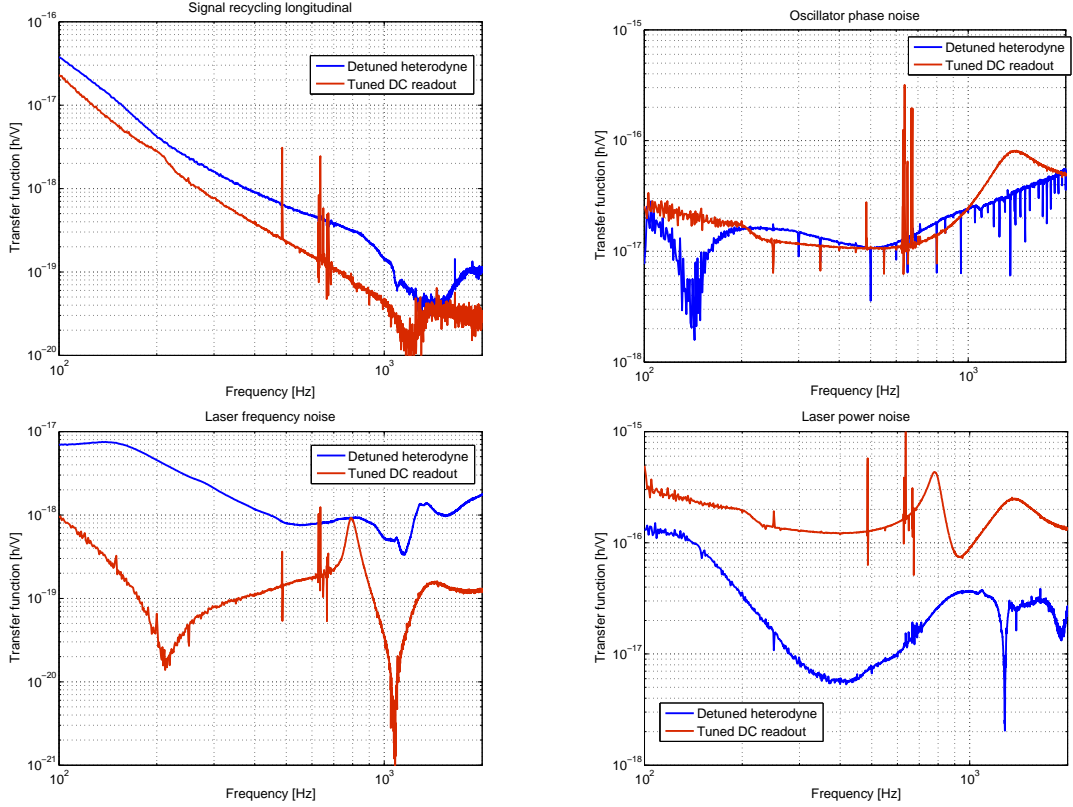


**Figure 3.** Comparison of the noise transfer functions to  $h$  between detuned heterodyne (blue curves) and tuned DC readout (red curves). The peaks in the noise transfer function for tuned DC readout at 785 Hz and 1365 Hz are due to the resonance in the signal recycling cavity of respectively, the signal recycling control sidebands and the Michelson control sidebands. Such peaks will be eliminated after the addition of the output mode cleaner which prevents the control sidebands to reach the detection photodiode.

400 mW of total power will be available for detection at the dark port. To handle that amount of power, multiple photodiodes will have to be used and a large dark fringe offset will be required. To avoid this solution, an Output Mode Cleaner (OMC) will be installed, reducing the incident power on the detection photodiode by a factor 20.

The Output Mode Cleaner (OMC) is a filter cavity transmitting the DC field in the fundamental mode to the photodiode and attenuating the higher order modes and the modulation sidebands. The details of the OMC can be found in the following sections.

### 3.1. Requirements

The OMC must satisfy two main requirements:

- (i) The power of the RF sidebands at 15 MHz must be reduced by at least a factor 100 in transmission. This requirement tells us how selective the mode cleaner must be, so it gives us an upper limit on the mode cleaner bandwidth. Practically, for a light round trip length of 66 cm, this requirement is satisfied for a finesse above 150.
- (ii) The power of the higher order optical modes must be reduced by at least a factor 100 in transmission. This requirement sets a constraint on the finesse of the cavity and on the  $g$ -factor. With a finesse of 150, the requirement is met for a  $g$ -factor of 0.3 or 0.7,

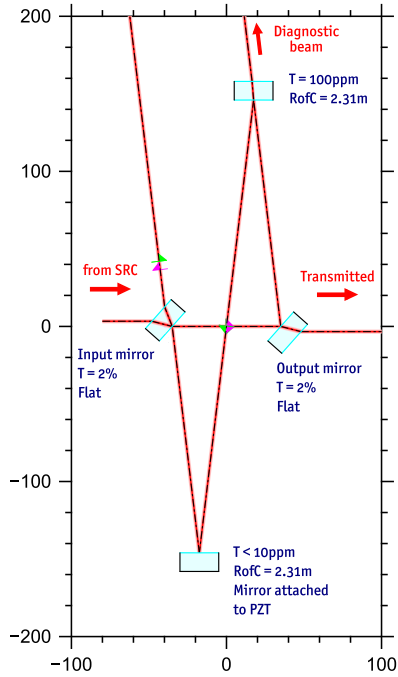


**Figure 4.** Optical setup of the OMC with the dimension in millimeter. The beam leaving the signal recycling cavity is coming from the left.

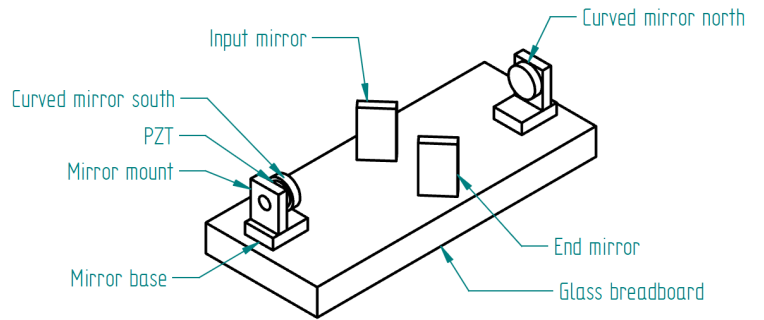


**Figure 5.** Isometric view of the OMC. All parts are mode of fused silica expect for the PZT.

for suppression of the higher order modes up to the 6<sup>th</sup> order and for an even number of mirrors in the cavity.

### 3.2. Optical and mechanical design

For the optical parameters of the OMC, we chose the minimal acceptable finesse i.e. 150. The preferred  $g$  factor is 0.735 which allows a larger beam size on the mirror than a  $g$  factor of 0.3.

The design of the OMC must also take into account that the optics will be installed on an isolated platform where the weight of the components must be carefully distributed. For this reason, the OMC is composed by 4 mirrors equally distributed on either side of the incoming beam as shown in the left part of figure 4. A 4-mirror configuration presents also two additional advantages: first the vertical and horizontal resonances are degenerate [11], so the number of optical mode resonances is halved compared to a mode cleaner with an odd number of mirrors. Second, the mirror which is not used for the input or output port and not glued to the opaque PZT can be partially transmissive, so a low power beam can exit the OMC and be used for diagnostic without the introduction of an additional beam splitter.

A piezo actuator (PZT) is glued to one of the curved mirror to control the length of the OMC. The PZT is composed of low voltage multi layer stack and will be used to longitudinally lock the OMC to the incoming fundamental mode. The control and the autoalignment of the OMC are detailed in the paper by M. Prijatelj et al. [8].

For thermal stability and low thermal noise, it was decided that all the parts of the OMC will be made of fused silica, except for the PZT. Instead of using a spacer, the optics are mounted on a rectangular cuboid glass breadboard. The input and output mirrors which are flat, have a rectangular shape, whereas the two curve mirrors are cylindrical.

The low frequency thermal drift of the optical path is further minimized since more than 70%

of the thermal expansion of the glass breadboard is compensated by the thermal expansion of the PZT for homogenous temperature change.

The glass breadboard is relatively thick, 38 mm. This dimension was optimized to minimize the nuisance of the mechanical modes which can modulate the optical path length of the OMC. In particular, the first mechanical mode of the OMC breadboard is chosen to be at 1.3 kHz where the sensitivity of the interferometer is already slightly degraded by the second harmonic of the violin modes of the suspension fibers.

The substrate for the optics is made of highly homogenous, low inclusion synthetic fused silica (Schott 7980-0-A), the optical mounts and mirror bases are made with a slightly lower quality fused silica (Schott 7980-3-C) and finally the glass breadboard is made of industry-grade fused silica (Schott Lithosil QT). The optics are superpolished and IBS coated. The other parts are simply polished. In the specification, special attention was drawn to the perpendicularity of the different surfaces to ensure a tilt free assembly.

### *3.3. Building and testing*

The different parts have been glued with the epoxy Optocast 3553-UTF-LV-HM. This UV-cured epoxy was particularly suitable since a very thin layer can be applied and it has very low residual outgassing. The mirrors were first positioned to their mounts using mechanical templates. The use of templates was inspired from the experience developed with the bonding of LISA pathfinder glass breadboard [12]. Since the epoxy is only cured after UV light is applied, all the parts can be accurately positioned without hurry. To position the mirrors on the glass breadboard, two steps were required. First a template was used to glue 3 out of the 4 OMC mirrors. Then to glue the last mirror, a carefully aligned laser was sent through the cavity and the last mirror was positioned manually to close the cavity.

The OMC is controlled via the LIGO Control and Data System (CDS) designed for Advanced LIGO. The error signal to keep the OMC on resonance is derived by dithering the PZT at 20 kHz and then demodulating the transmitted light in phase. Stable locks were achieved, in the AEI clean room with the feedback applied to the input laser. This setup is different from what is planned for GEO-HF, since for GEO-HF the feedback will be applied to the PZT itself [8]. Nevertheless, the test gave us some valuable insight and experience about the OMC and the LIGO CDS.

By scanning the cavity over one free spectral range, two essential parameters of the OMC cavity can be derived. First, the finesse of the cavity, derived from the measurement of the cavity linewidth was found to be 147, and second, the g-factor, derived from the frequency spacing of the higher order modes was measured to be 0.731. Both the finesse and the g factor are within 2% of the design value.

## **4. Conclusion and outlook**

A DC readout control scheme has been implemented for the GEO600 interferometer. The preliminary sensitivity achieved without an output mode cleaner is comparable to heterodyne readout in the middle frequency range (100 Hz - 300 Hz) and at high frequency ( $\geq 2$  kHz). In parallel to this work, an output mode cleaner has been build and tested off site. The output mode cleaner actuator is controlled by the LIGO CDS system, showing the path for further digital implementation in GEO.

As of September 2009, the plan is to first have a short commissioning of DC readout without the OMC, then inject squeezed vacuum from the dark port and finally around mid-autumn,

install the OMC in vacuum in front of the DC readout photodiode. Only then, intensive commissioning and optimization of tuned DC readout for GEO-HF will be endeavored.

## Acknowledgments

We would like to thank R. Schilling for his precious help with Optocad and the design of the OMC. We also thank Sam Waldman for useful comments on this manuscript. The authors are grateful for support from the Science and Technology Facilities Council (STFC) in the UK, the BMBF, Max Planck Society (MPG) and the state of Lower Saxony in Germany and the European Gravitational Observatory (EGO). This work was partly supported by DFG grant SFB/Transregio 7 "Gravitational Wave Astronomy". This document has been assigned LIGO Laboratory document number LIGO-P0900119.

## References

- [1] Grote H (for the LIGO Scientific Collaboration) 2008 *Classical and Quantum Gravity* **25** 114043
- [2] Willke B, Ajith P, Allen B, Aufmuth P, Aulbert C, Babak S, Balasubramanian R, Barr B W, Berukoff S, Bunkowski A, Cagnoli G, Cantley C A, Casey M M, Chelkowski S, Chen Y, Churches D, Cokelaer T, Colacino C N, Crooks D R M, Cutler C, Danzmann K, Dupuis R J, Elliffe E, Fallnich C, Franzen A, Freise A, Gholami I, Gossler S, Grant A, Grote H, Grunewald S, Harms J, Hage B, Heinzl G, Heng I S, Hepstonstall A, Heurs M, Hewitson M, Hild S, Hough J, Itoh Y, Jones G, Jones R, Huttner S H, Kotter K, Krishnan B, Kwee P, Lück H, Luna M, Machenschalk B, Malec M, Mercer R A, Meier T, Messenger C, Mohanty S, Mossavi K, Mukherjee S, Murray P, Newton G P, Papa M A, Perreux-Lloyd M, Pitkin M, Plissi M V, Prix R, Quetschke V, Re V, Regimbau T, Rehbein H, Reid S, Ribichini L, Robertson D I, Robertson N A, Robinson C, Romano J D, Rowan S, Rudiger A, Sathyaprakash B S, Schilling R, Schnabel R, Schutz B F, Seifert F, Sintes A M, Smith J R, Sneddon P H, Strain K A, Taylor I, Taylor R, Thuring A, Ungarelli C, Vahlbruch H, Vecchio A, Veitch J, Ward H, Weiland U, Welling H, Wen L, Williams P, Winkler W, Woan G and Zhu R 2006 *Classical and Quantum Gravity* **23** S207–S214
- [3] Hild S, Grote H, Degallaix J, Chelkowski S, Danzmann K, Freise A, Hewitson M, Hough J, Lück H, Prijatelj M, Strain K A, Smith J R and Willke B 2009 *Classical and Quantum Gravity* **26** 055012
- [4] Hild S, Grote H, Hewitson M, Lück H, Smith J R, Strain K A, Willke B and Danzmann K 2007 *Classical and Quantum Gravity* **24** 1513–1523
- [5] Chelkowski S, Vahlbruch H, Hage B, Franzen A, Lastzka N, Danzmann K and Schnabel R 2005 *Physical Review A* **71** 013806
- [6] Ward R L, Adhikari R, Abbott B, Abbott R, Barron D, Bork R, Fricke T, Frolov V, Heefner J, Ivanov A, Miyakawa O, McKenzie K, Slagmolen B, Smith M, Taylor R, Vass S, Waldman S and Weinstein A 2008 *Classical and Quantum Gravity* **25** 114030
- [7] Grote H 2009 Status of GEO600 LIGO Technical Document No. P0900199, submitted to CQG
- [8] Prijatelj M, Grote H, Degallaix J, Hewitson M, Hild S, Affeldt C, Freise A, Leong J, Lück H, Strain K A, Wittel H, Willke B and Danzmann K 2009 Control and automatic alignment of the output mode cleaner of GEO 600 LIGO Technical Document No. P0900156, submitted to JPCS
- [9] Lück H, Affeldt C, Degallaix J, Freise A, Grote H, Hewitson M, Hild S, Leong J, Prijatelj M, Strain K, Willke B, Wittel H and Danzmann K 2009 The transition to GEO-HF LIGO Technical Document No. P0900122, submitted to JPCS
- [10] Smith J R, Degallaix J, Freise A, Grote H, Hewitson M, Hild S, Lück H, Strain K A and Willke B 2008 *Classical and Quantum Gravity* **25** 035003
- [11] Barriga P, Zhao C and Blair D G 2005 *General Relativity and Gravitation* **37** 1609–1619
- [12] Middleton K F, Caldwell M E, Edeson R, Neeson C, Munro G, Eley C, Sandford M, Braxmaier C, Johann U, Killow C, Robertson D, Ward H, Hough J, Heinzl G and Wand V 2006 *Optical Engineering* **45** 125601